BMC Pharmacology and Toxicology

RESEARCH

Open Access

Kaempferol inhibits cardiomyocyte pyroptosis via promoting O-GlcNAcylation of GSDME and improved acute myocardial infarction

Jie Zhou[1], Huifei Zhou[1], Jianfeng Zhu[1] and Shunjin Fang[1*]

Abstract

Acute myocardial infarction (AMI) is a leading fatal cardiovascular disease and poses a major threat to human health. Pyroptosis, an inflammation-related programmed cell death, plays a critical role in the progression of AMI. Kaempferol is a natural flavonoid compound with a variety of pharmacological effects, which exerts a significant cardioprotective function. The role of O-GlcNAcylation, a post-translation modification, has received attention in diseases including AMI. In this research, we explored the therapeutic potential of Kaempferol to AMI due to its well-known cardioprotective effect, including its antioxidant and anti-inflammatory properties. Hypoxia/reoxygenation (H/R) model was adopted to provoke myocardial injury and AMI mice model was established. Our findings indicated that H/R lessened cell viability and contributed to the release of LDH, IL-1β and IL-18, cell pyroptosis rate, and the expression of NLRP3, active caspase 1 and GSDMD-N-terminal domain (GSDMD-N). Kaempferol mitigated myocardial damage caused by H/R through repressing cell pyroptosis. Besides, we discovered that Kaempferol restored the levels of O-GlcNAcylation by regulating the activity of OGT (O-GlcNAc transferase) and OGA (O-GlcNAcase) in H/R-treated H9c2 cells. Notably, molecular docking revealed the binding relationship between Kaempferol and OGT. Further, we proved that knockdown of OGT abrogated the function of Kaempferol in H/R-induced pyroptosis. In AMI mice, Kaempferol relieved the myocardial tissue injury and decreased the NLRP3 and GSDME-N protein levels. More importantly, our results illustrated that OGT was responsible for the O-GlcNAcylation of GSDME at T94 site and acted as an inducing factor for GSDME phosphorylation. Namely, this study validated that Kaempferol facilitated GSDME O-GlcNAcylation to inhibit H/R-induced pyroptosis in an OGT-dependent manner.

Keywords Acute myocardial infarction, Kaempferol, Pyroptosis, O-GlcNAcylation, GSDME

*Correspondence:
Shunjin Fang
SJFangdr@163.com
[1]Department of Critical Care Medicine, Huzhou Third Municipal Hospital, Huzhou, Zhejiang 313000, China

Introduction

Acute myocardial infarction (AMI) is one of the common and fatal heart diseases worldwide with an increasing incidence [1]. Based on epidemiological data, it is estimated that there are approximately 10,000 newly diagnosed cases globally [2]. This disease has been documented to often affect patients with older age [3]. With the aggravation of aging population, the prevalence of AMI is expected to rise further, resulting in a huge burden on the public health system [4]. Despite advances in diagnostic techniques, AMI remains underdiagnosed, with approximately 2–6% of patients not receiving a correct diagnosis [5]. Furthermore, AMI is closely linked to other cardiovascular diseases (CVDs), such as hypertension, atherosclerosis, and heart failure, which often coexist and exacerbate the condition [6]. Although AMI is an acute event, it can have long-term effects on both the physical and psychological health of patients [7]. AMI caused by reduced cardiac blood perfusion leads to insufficient cardiac oxygen supply and aberrant myocardial energy metabolism [8]. Given that the mechanism of AMI is still obscure, investigating its pathogenesis and identifying latent preventive measures and pharmacological agents are urgently needed to improve the current status of AMI therapy.

3,4′,5,7-tetrahydroxyflavone, commonly termed Kaempferol, is a natural flavonoid compounds widely existed in a wide range of plants, including tea, beans, fruits and vegetables [9]. Kaempferol, originating from the rhizome of Kaempferia, has been shown to possess diverse pharmacological effects, such as anti-inflammation, antibiosis, antioxidant, antibacterial activity, anti-tumor potency and cardioprotection [10, 11]. Accumulating investigations have expounded that Kaempferol exhibits a significant improvement in cardiovascular diseases, which is attributed to its role in inhibiting oxidation, inflammation, apoptosis and fibrosis, regulating calcium and mitochondrial function, thus ameliorating the structure and function of the heart [12, 13]. Notably, the cardioprotective potential of Kaempferol has been verified [14], but its molecular mechanism remains to be elucidated.

Pyroptosis is a newly discovered form of inflammation-mediated programmed cell death [15]. Unlike cell apoptosis, which depends on caspase 3, pyroptosis is dependent on the persistent activation of caspase 1 [16]. It is widely recognized that NLRP3 inflammasome serves as a critical inducer for pyroptosis, which contributes to the generation of mature caspase 1 and provokes the massive release of interleukin-1β (IL-1β), IL-18 and other inflammatory factors, leading to gasdermin-dependent cell disruption, intense inflammatory response and eventual pyroptosis [17, 18]. In recent years, pyroptosis is participated in a variety of pathological processes, including myocardial damage after AMI [19]. Overactivation of pyroptosis brings about sustained loss of cardiomyocytes, the augment of infarct size and poor cardiac remodeling in the development of AMI [20]. Emerging evidence suggests that suppressing pyroptosis attenuates myocardial injury caused by AMI through lessening infarct size and improving heart dysfunction [21]. On the basis of the above facts, targeting the pyroptosis pathway may represent a novel intervention for the treatment of AMI. Up to now, Kaempferol has been demonstrated to perform inhibitory effects on cell pyroptosis in multiple diseases, such as glioblastoma [22], Parkinson's disease [23] and spinal cord injury [24]. Despite the amelioration effect of Kaempferol on AMI [25], the mechanism of its action is complex and has not yet been well documented, and its regulatory effect on pyroptosis of myocardial cells remains unknown. Hence, this research is purposed to determine the effect of Kaempferol on cardiomyocyte pyroptosis in AMI and shed light on its underlying drug mechanism.

Methods

Cell culture

Rat myocardial cell line H9c2 was purchased from American Type Culture Collection (ATCC, USA). This cell line was used because it has well-established relevance in cardiovascular research and is able to mimic the response of primary cardiomyocytes to injury, and it is easier to culture and manipulate than primary cardiomyocytes. On the basis of product manuals, cells were grown in culture medium consisting of DMEM (Gibco, USA), 10% FBS (Gibco, USA) and 1% penicillin/streptomycin (Sigma-Aldrich, USA) and cultivated at 37 ℃ under the air of 5% CO_2. The fresh medium was changed every 2–3 days. H9c2 cells were collected until cell confluence reached 80–90%.

Hypoxia/reoxygenation model

To simulate myocardial ischemia in vitro, cardiomyocytes were subjected to hypoxia/reoxygenation (H/R) treatment. Briefly, H9c2 cells were maintained in a hypoxia atmosphere of 1% O_2, 94% N_2 and 5% CO_2 for 16 h and then reoxygenated for 2 h under the normoxic conditions (95% air and 5% CO_2) [26].

Cell transfection and treatment

For silencing of OGT, small interfering RNAs (siRNAs) targeting OGT (si-OGT#1/2) were designed by GenePharma (Guangzhou, China) with non-specific siRNAs as the negative control. To upregulate OGT, vectors expressing OGT (pCMV-OGT) were also acquired from GenePharma. These plasmids were transfected into H9c2 cells by utilization of Lipofectamine 3000 (Invitrogen, USA). In order to estimate the potential of Kaempferol,

H9c2 cells were treated with 5, 10, and 20 μM Kaempferol for 2 h before reoxygenation. After reoxygenation, the cells were harvested.

Animal experiment

Eighteen 8-week-old C57/BL6 mice were purchased from Charles River Laboratories (Beijing, China) and randomized into three groups using a random number table: Sham operation group, Model group, and Model + Kaempferol group, with six mice in each group, balanced for gender. Mice in all groups except the Sham operation group underwent electrocardiogram (ECG) lead attachment, tracheal intubation, and connection to a small animal ventilator, set to ventilate at a frequency of 150 breaths per minute with an inspiration-to-expiration ratio of 5:4. A thoracotomy was performed at the third and fourth intercostal space on the left side to expose the heart. With the left coronary artery as a landmark between the left atrial appendage and the pulmonary arterial cone, the left anterior descending artery (LAD) was permanently ligated using 8 – 0 sutures. Success of ligation was confirmed by observing ST-segment elevation on ECG lead II and visually identifying tissue whitening distal to the ligation site, indicative of myocardial ischemia. The chest was then closed in layers. The Sham operation group underwent thoracotomy without LAD ligation. The Kaempferol group received a daily oral gavage of kaempferol at a dose of 50 mg/kg/day [27] for six consecutive weeks. Control and Model groups were given an equal volume of distilled water at 10 mL/kg/day. At the end of the treatment, all mice were euthanized by intraperitoneal injection of pentobarbital sodium (160 mg/kg). Myocardial tissues were harvested for histological examination with Hematoxylin-Eosin (H&E) staining and Western blot analysis.

H&E staining

For assessment of myocardial tissue injury, hematoxylin and eosin (H&E) staining was performed on harvested mouse heart samples. Briefly, excised hearts were fixed in 4% paraformaldehyde, followed by dehydration through a graded ethanol series and embedding in paraffin. Transverse sections of 5-μm thickness were cut and mounted on glass slides. After deparaffinization and rehydration, the sections underwent hematoxylin staining for 5 min, washed, and then counterstained with eosin for 1 min. Following dehydration and coverslipping, the slides were examined under light microscopy to evaluate morphological changes indicative of myocardial damage, including inflammatory cell infiltration, necrosis, and structural abnormalities.

Detection of myocardial injury markers

To quantify cardiac-specific markers in myocardial tissue, creatine kinase MB isoenzyme (CK-MB) and cardiac troponin I (cTnI) were measured using commercially available enzyme-linked immunosorbent assay (ELISA) kits according to the manufacturers' instructions. Briefly, frozen myocardial tissues were homogenized in provided lysis buffer, and the supernatant was collected after centrifugation. Standards and tissue lysate samples were added to the respective wells of a pre-coated microplate, followed by sequential incubations with detection antibodies and substrate solutions. Color development was proportional to the concentration of CK-MB and cTnI present. Absorbance was read at specific wavelengths using a microplate reader, and the concentrations of CK-MB and cTnI were determined from the standard curves.

Transthoracic echocardiography

Mice were anesthetized with 1.5% isoflurane inhalation. The cardiac function was detected using the Vevo2100 imaging system (VisualSonics). M-mode images were recorded. Ejection fraction (EF) and fractional shortening (FS) were detected.

Cell proliferation assay

Following corresponding treatments, H9c2 cells were seeded into a 96-well plate at a density of 5×10^3 cells/well. In line with the guidelines provided by the supplier, H9c2 cells were treated with the Cell Count kit-8 (CCK-8) reagent (Dojindo, Japan) and subjected to 2 h of incubation at 37 ℃. Absorbance was examined at 450 nm for detection of cell viability.

Detection of LDH release

LDH activity in the cells or myocardial tissue was tested using an LDH assay kit (R&D Systems, USA) according to the product manuals. Optical density was determined by a plate reader at 490 nm and 690 nm, and the LDH level was calculated on the basis of the recommended formula and standard curve.

Flow cytometry

For identification of cell pyroptosis rate, flow cytometry was adopted to examine the activation level of caspase-1 using the caspase-1 Detection Kit (ImmunoChemistry, USA). In this kit, Tyr-Val-Ala-Asp (YVAD) was a caspase-1 inhibitor that could bind to caspase-1. YVAD was labelled using fluorescein (FAM) dye and linked to fluoromethyl ketone (FMK). In conformity with the recommendations supplied by the manufacturer, FAM-YVAD-FMK was diluted using PBS at a ratio of 1:5. H9c2 cells were collected and incubated with the diluted FAM-YVAD-FMK at 37 ℃ for 1 h to mark active caspase-1

enzyme. After washing, H9c2 cells were stained with propidium iodide (PI) and pyroptosis was detected by a FACS Aria III cytometer (BD CANTO, USA). The pyroptosis rate was calculated by double positive staining of FAM-YVAD-FMK and PI.

Enzyme-linked immunosorbent assay (ELISA)

H9c2 cells were subjected to matched treatments, followed by centrifugation at 4 ℃ for 10 min at 10,000 × g and there with measured with the commercial ELISA kits for IL-1β and IL-18 (R&D Systems) according to the product guidelines. Finally, absorbance was detected with a plate reader at the wavelength of 450 nm for examination of cytokine concentrations.

Real-time quantitative PCR (RT-qPCR) assay

In line with the supplier's directions, the TRIzol® reagent (Invitrogen) was applied for isolation of total RNA from H9c2 cells. Following reverse transcription using the RevertAid™ cDNA Synthesis kit (Takara, Japan), cDNA samples were subjected to RT-qPCR analysis in ABI 7500 Real-Time PCR system (Applied Biosystems, USA) by means of the SYBR® Green Supermix kit (Bio-Rad, USA). The sequences of adopted primers were listed: OGT, forward: 5′-CCTGGGTCGCTTGGAAGA-3′ and reverse: 5'-TGGTTGCGTCTCAATTGCTTT-3'; β-actin, forward: 5′-AGGGAAATCGTGCGTGAC-3′ and reverse, 5′-CGCTCATTGCCGATAGTG-3′. The relative expression of OGT was calculated with the $2^{-\Delta\Delta Ct}$ method and presented by normalization to β-actin.

Western blot

Protein extracts from H9c2 cells or myocardial tissues were acquired with RIPA lysis buffer, quantitated by a bicinchoninic acid protein assay kit (Beyotime, China) and loaded on 12% SDS-PAGE. Following transferring onto PVDF membranes, the bands were sealed in 5% non-fat milk, probed by corresponding primary antibodies overnight at 4 ℃ and treated with HRP-labeled secondary antibodies for 1.5–2 h at room temperature. Afterwards, the blots were detected using the Tanon 2000 Imaging System (Tanon, China) utilizing the chemiluminescence kit (Beyotime). The following primary antibodies were applied in western blot: anti-NLRP3 (Abcam, USA), anti-caspase 1-p20 (Abcam), anti-GSDMD-N (Abcam), anti-GSDME-N (Abcam), anti-phosphoserine/threonine (BD Biosciences, USA), anti-*O*-Linked N-acetylglucosamine (anti-O-GlcNAc; i.e. anti-RL2; Abcam) and anti-GAPDH (Abcam). GAPDH was employed as the internal control. The results were quantified using the ImageJ software.

Molecular docking

According to the three-dimensional structure of Kaempferol and potential target proteins downloaded from the Protein Data Bank database. AutoDock tools (ADT) and AutoGrid tool were employed to identify the docking position of Kaempferol and target protein with the aid of the Lamarckian genetic algorithm (LGA).

Surface plasmon resonance (SPR) analysis

SPR analysis was performed using the Biacore-X100 instrument (Cytiva) with CM5 sensor chip according to a previous study [28].

Protein O-GlcNAcylation level detection

Immunoprecipitation was performed using the IP/co-IP kit (Absin). H9c2 cells were lysed using IP lysis buffer at 4 ℃ and centrifuged at 14,000 ×g for 10 min. The lysate was incubated with 5 μg anti-RL2 at 4 ℃ overnight and incubated with 5 μL protein A and 5 μL protein G at 4 ℃ for 3 h. After centrifugation at 12,000 ×g for 1 min, the sediments were washed four times with wash buffer. Then, the sediments were suspended in SDS buffer and heated at 100℃ for 5 min for SDS-PAGE. Western blot was conducted to measure NLRP3, caspase1, GSDMD, and GSDME.

Statistical analysis

Data processing was performed with GraphPad Prism version 8.0 (GraphPad software, USA). All experimental results were expressed as mean ± standard deviation from three repeated assays. Difference between two groups was estimated by Student's *t*-test. Comparison of more than two groups was analyzed using ANOVA and post-hoc Tukey's test. Statistical significance was set as $P < 0.05$.

Results

Kaempferol alleviated the pyroptosis of H/R-induced cardiomyocytes

First, we ascertained the effect of Kaempferol in myocardial damage caused by H/R. According to the molecular structure displayed in Fig. 1A, Kaempferol was 3,5,7-trihydroxy-2-(4-hydroxyphenyl)-4 H-1-benzopyran-4-one. Then, H9c2 cells were induced by H/R to mimic AMI injury and stimulated by Kaempferol (Fig. 1B). CCK-8 assay was conducted to investigate the impacts of Kaempferol on the viability of H/R-treated H9c2 cells. It was observed that H/R injury resulted in the reduction of cell viability and Kaempferol at the concentrations of 10 μM and 20 μM significantly elevated cell viability (Fig. 1C). Subsequently, our findings disclosed that the increase of LDH activity caused by H/R was recovered by Kaempferol (Fig. 2A), suggesting that Kaempferol attenuates cell damage caused by H/R. Pyroptosis is a form of

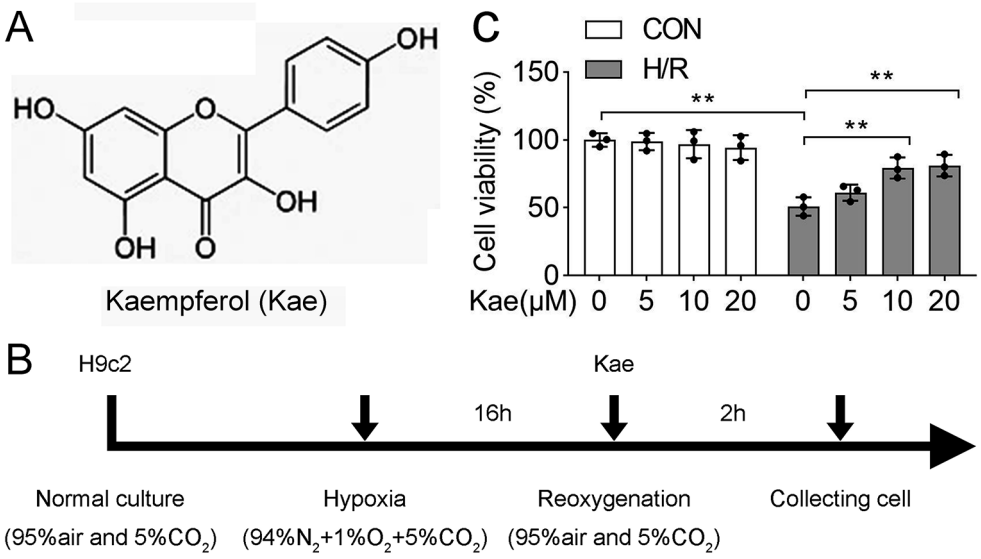

Fig. 1 Kaempferol decreased cell proliferation following H/R treatment. (**A**) The molecular structural formula of Kaempferol. (**B**) Flow chart of cell experimental design. (**C**) H9c2 cells were induced by H/R and treated with 0, 5, 10, and 20 μM Kae, and then CCK-8 assay was performed to evaluate cell viability. CON, control; H/R, hypoxia/reoxygenation; Kae, Kaempferol. $^{**}P < 0.01$

inflammatory cell death, characterized by the rupture of the cell membrane, leading to the release of intracellular contents and triggering a strong inflammatory response. To investigate whether Kaempferol mainly acts on pyroptosis rather than other types of programmed cell death, we performed western blot to measure several proteins associated with apoptosis, necrosis, and autophagy. We found that Kaempferol did not significantly affect the levels of caspase3, PARP1, RIPK1, RIPK3, and LC3-II/LC3-I (Figure S1), suggesting that Kae had no significance on apoptosis, necrosis, and autophagy. Thus, we assessed pyroptosis. Besides, we demonstrated that H/R facilitated the release of IL-1β and IL-18, and Kaempferol restored the levels of IL-1β and IL-18 (Fig. 2B-C). Flow cytometry analysis indicated that H/R stimulation promoted the activation of caspase 1 and Kaempferol repressed the pyroptosis rate of H/R-treated H9c2 cells (Fig. 2D). Likewise, western blot revealed that the enhancement of NLRP3, active caspase 1 (p20) and GSDMD-N expression triggered by H/R was abolished by treatment with Kaempferol (Fig. 2E). Collectively, Kaempferol attenuated H/R-induced cell pyroptosis.

Kaempferol promoted OGT-mediated O-GlcNAcylation in H/R-treated cardiomyocytes

Considering the involvement of O-GlcNAcylation in myocardial injury, we then explored the role of Kaempferol in O-GlcNAcylation. Western blot results showed that the O-GlcNAcylation of H/R-treated H9c2 cells was lower than that of the control group, and Kaempferol markedly elevated O-GlcNAcylation following H/R stimulation (Fig. 3A). Consistently, we found that H/R caused the decreased OGT level and heightened expression of OGA, while Kaempferol only reversed the downregulation of OGT but failed to affect OGA expression in H/R-induced cells (Fig. 3A). Molecular docking results illustrated that Kaempferol could effectively bind to the active pocket of OGT, suggesting that Kaempferol exhibited strong spontaneous hydrogen bond interaction with OGT (Fig. 3B-D). SPR analysis results showed that the binding affinity (KD) was 0.82 μM, indicating the direct interaction between Kaempferol and OGT (Fig. 3E and F). On the basis of foregoing findings, we concluded that OGT was responsible for the regulatory effect of Kaempferol in O-GlcNAcylation of H9c2 cells treated with H/R.

Knockdown of OGT reversed the inhibitory effects of Kaempferol on H/R-induced pyroptosis

In order to identify the participation of OGT in the role of Kaempferol, OGT was silenced in H/R-induced H9c2 cells following treatment with Kaempferol. RT-qPCR and western blot assay proved that the mRNA and protein levels of OGT were downregulated by transfection with si-OGT#1 or si-OGT#2 (Fig. 4A and B). According to these results, si-OGT#1 transfected cells were used in the following experiments. Our observations manifested that Kaempferol prominently suppressed LDH activity and the secretion of IL-1β and IL-18 in H9c2 cells treated with H/R, whereas knockdown of OGT relieved this suppressive effect (Fig. 4C-E). Additionally, flow cytometry illuminated that Kaempferol abated the elevation of caspase 1 activation induced by H/R, and silencing of OGT abrogated the influences of Kaempferol on cell pyroptosis rate (Fig. 4F). In concert with these findings, we justified that increased NLRP3, caspase 1-p20 and GSDMD-N levels caused by H/R stimulation were remarkably

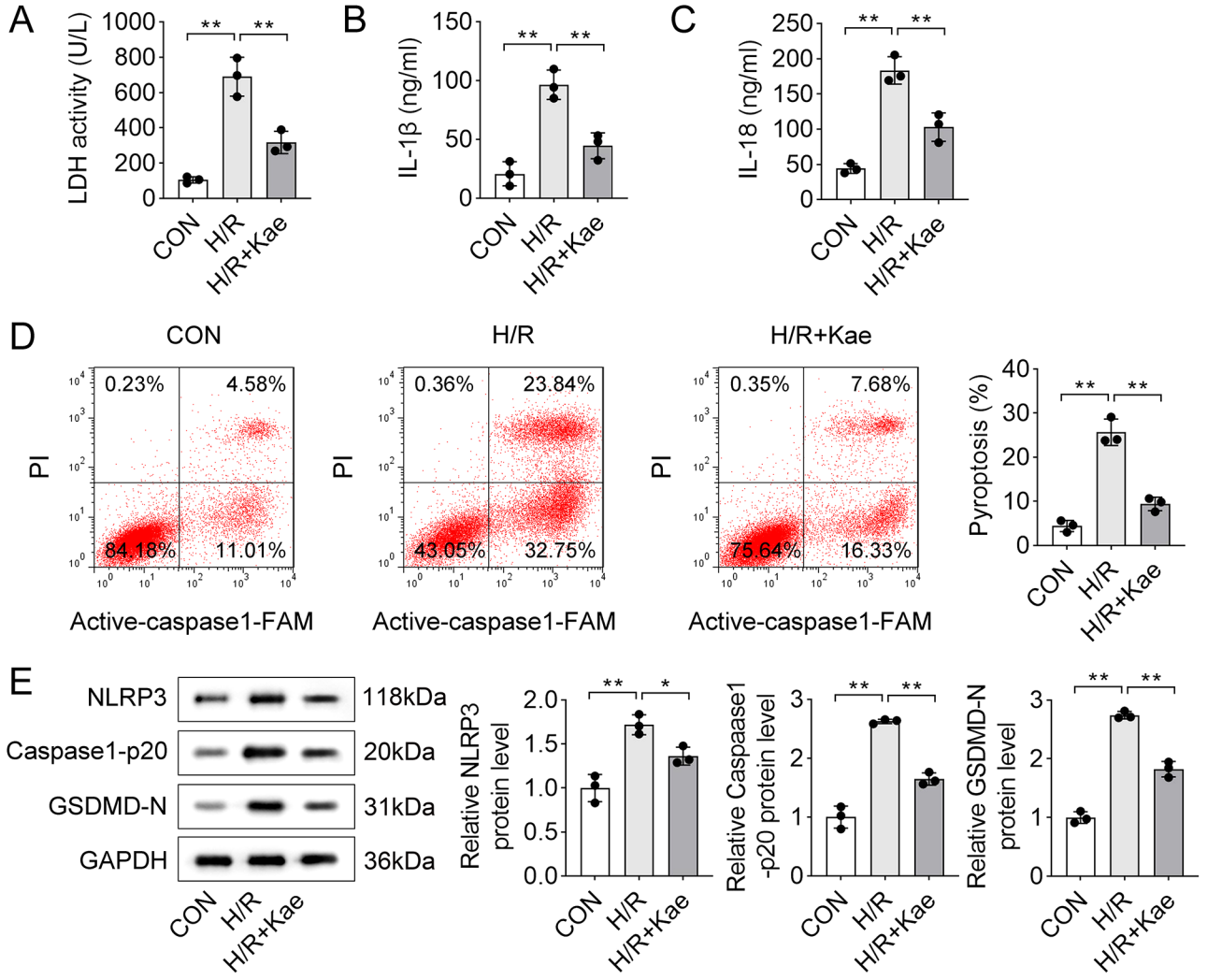

Fig. 2 Kaempferol restrained H/R-induced cell pyroptosis. For identifying the effects of Kaempferol on cell pyroptosis, H9c2 cells stimulated with H/R to induce injury, and were administered with 20 μM Kaempferol (**A**) LDH release was measured with LDH detection assay. The concentrations of (**B**) IL-1β and (**C**) IL-18 were examined by ELISA assays. (**D**) Flow cytometry was carried out to analyze cell pyroptosis rate. (**E**) Western blot analysis of the expression of pyroptosis markers NLRP3, caspase 1-p20 and GSDMD-N. CON, control; H/R, hypoxia/reoxygenation; Kae, Kaempferol; LDH, lactate dehydrogenase; IL-1β, interleukin-1β; IL-18, interleukin-18; PI, propidium iodide; GSDMD-N, GSDMD-N-terminal domain. $^{**}P < 0.01$. $^{*}P < 0.05$

reduced by Kaempferol, and downregulation of OGT countermanded the inhibition of indicated pyroptosis-related proteins by Kaempferol (Fig. 4G). Taken together, our findings indicated that Kaempferol exerted its cardioprotective function in H/R-treated H9c2 cells via enhancing OGT expression.

OGT functioned as a suppressing factor for GSDME cleavage via increasing its O-GlcNAcylation

Then, we further probed the modulatory mechanism governing OGT in H/R injury. Western blot assay was implemented to inquire the O-GlcNAcylation levels of pyroptosis markers in response to OGT overexpression using its overexpression vectors or knockdown using si-OGT#1. It was uncovered that upregulation of OGT increased OGT and O-GlcNAc levels, facilitated the O-GlcNAcylation of GSDME, while knockdown of OGT got the opposite results. However, OGT failed to affect the O-GlcNAcylation levels of NLRP3, caspase 1 and GSDMD (Fig. 5A). Meanwhile, silencing of OGT obviously weakened GSDME O-GlcNAcylation and there was no significant change in the O-GlcNAcylation modifications of NLRP3, caspase 1 and GSDMD, which suggested that GSDME might be the latent downstream effector for OGT (Fig. 5A). By employment of bioinformatics tool GlycoMine website, we determined the potential O-GlcNAcylation sites of GSDME (Fig. 5B). Accordingly, the top 4 predicted sites were mutated to determine the O-GlcNAcylation locus of GSDME. As shown in Fig. 5C and D, only mutation of T94 site overtly lessened the total O-GlcNAc, p-GSDME, and GSDME O-GlcNAcylation levels and heightened the cleavage of GSDME, validating

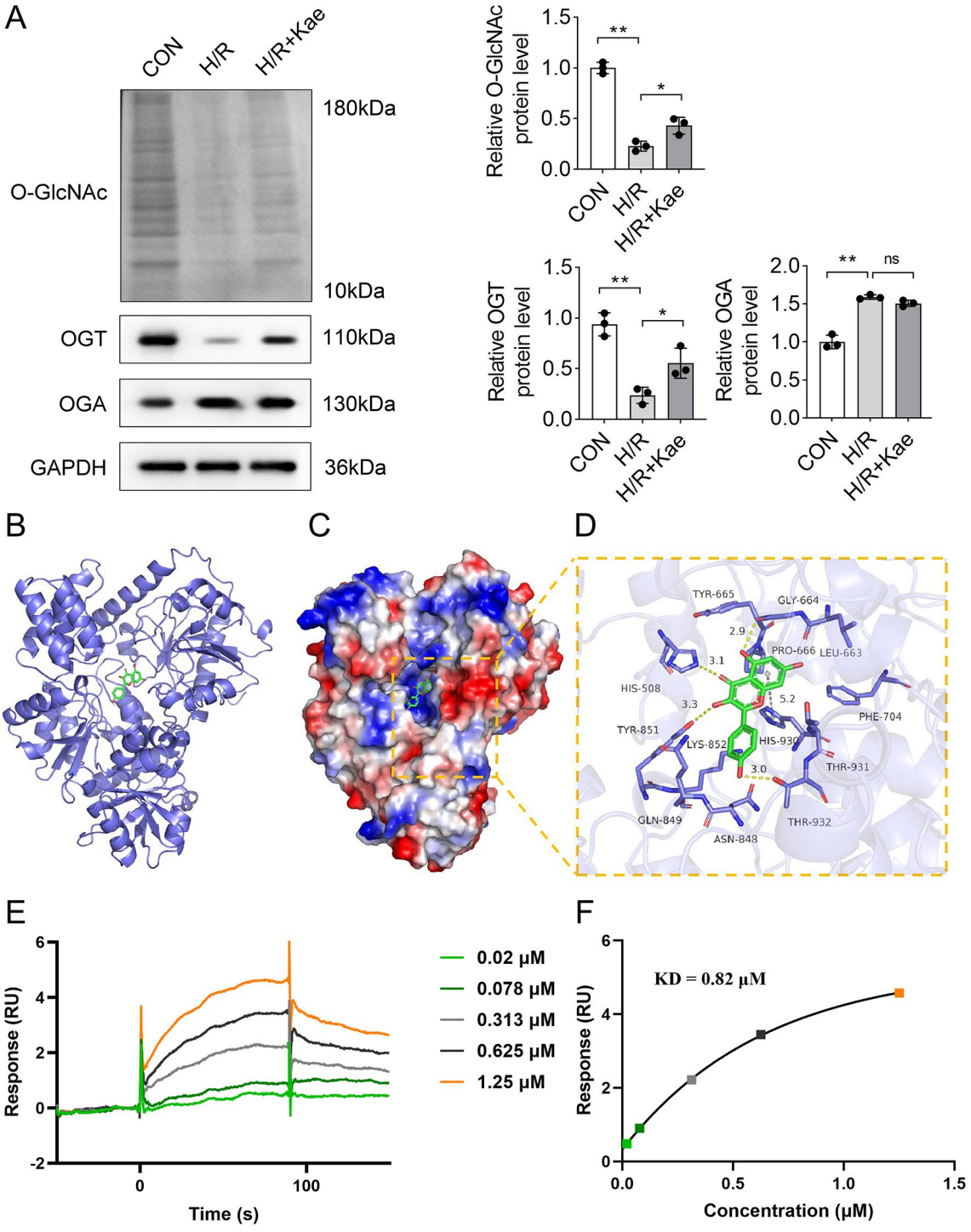

Fig. 3 Kaempferol promoted OGT-mediated O-GlcNAcylation in H/R-treated cardiomyocytes. (**A**) Following different treatments, western blot was conducted to detect O-GlcNAcylation level and the expression of OGT and OGA. (**B**-**D**) Molecular docking results confirmed the strong hydrogen bonding between Kaempferol and OGT. (**E**, **F**) SPR analysis was performed to verify the binding between Kaempferol and OGT. CON, control; H/R, hypoxia/reoxygenation; Kae, Kaempferol; SPR, Surface plasmon resonance. $^{**}P < 0.01$. $^{*}P < 0.05$. ns: no significance

that O-GlcNAcylation of GSDME at T94 was mediated by OGT. Notably, we discovered that overexpression of OGT promoted the phosphorylation of GSDME and weakened the expression of GSDME-N, while silencing of OGT produced the opposite results (Fig. 5E). These findings provided strong evidence that OGT induced GSDME phosphorylation to inhibit the cleavage of GSDME through promoting its O-GlcNAcylation.

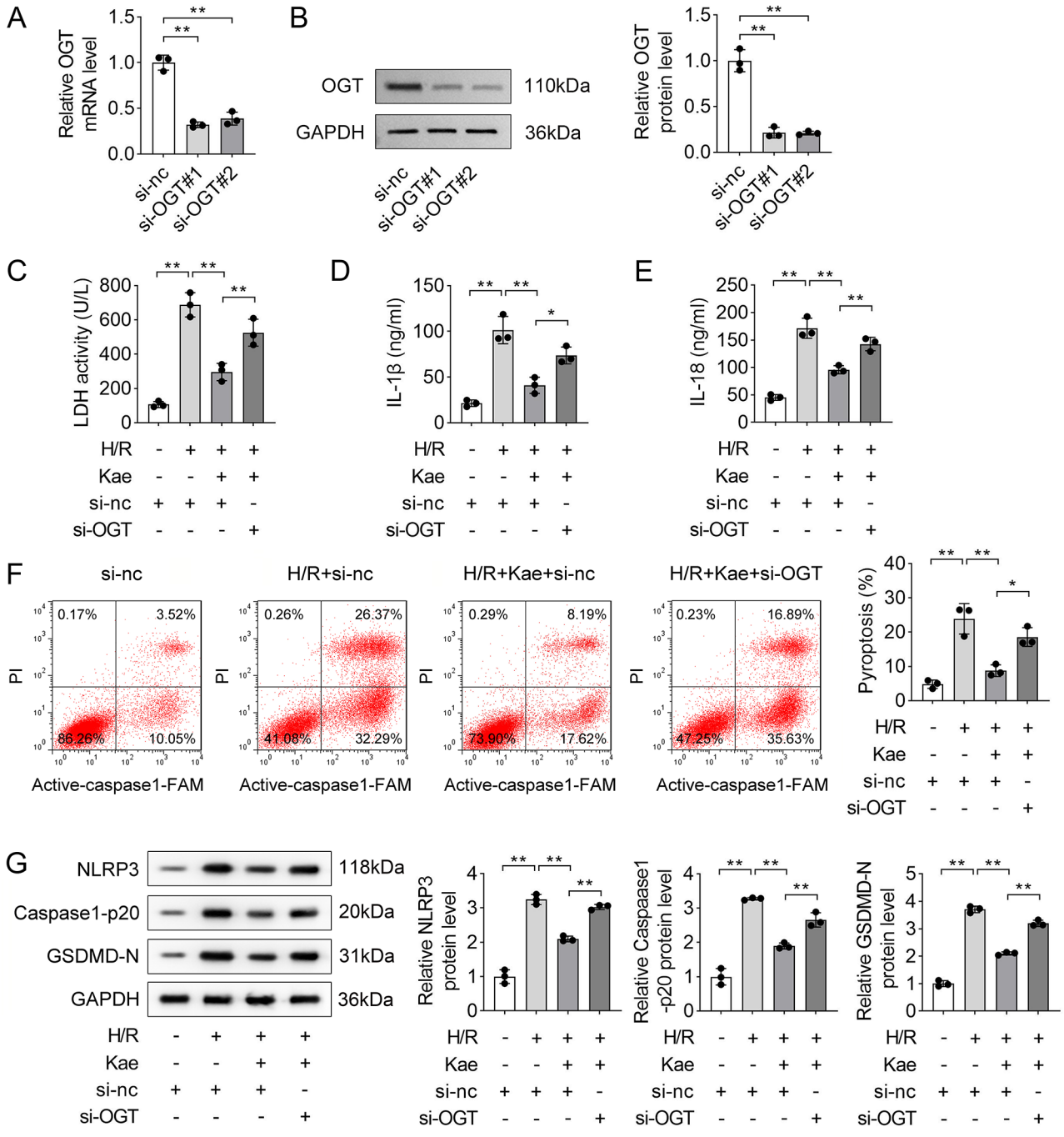

Fig. 4 Knockdown of OGT reversed the inhibitory effects of Kaempferol on H/R-induced pyroptosis. (**A**, **B**) The RT-qPCR and western blot detection of OGT expression in H9c2 cells transfected with si-nc or si-OGT#1/2. (**C**) LDH activity and the expression of (**D**) IL-1β and (**E**) IL-18 were examined by using corresponding kits. (**F**) The percent of pyroptotic cells was estimated by flow cytometry following different treatments. (**G**) The role of OGT in Kaempferol-mediated pyroptosis was also validated by western blot. si-OGT, small interfering RNA targeting OGT; si-nc, siRNA negative control; LDH, lactate dehydrogenase; IL-1β, interleukin-1β; IL-18, interleukin-18; PI, propidium iodide; GSDMD-N, GSDMD-N-terminal domain. $^{*}P < 0.05$, $^{**}P < 0.01$

Kaempferol alleviated the AMI progression in vivo

Finally, we establish the AMI model in vivo. We found that LDH (Fig. 6A), CK-MB (Fig. 6B) and cTnI (Fig. 6C) levels were increased in the myocardial tissues of AMI mice. Kaempferol treatment significantly decreased them. EF and FS were lower in the AMI mice than that in the sham mice, suggesting AMI induces cardiac dysfunction, while Kaempferol reversed the poor cardiac function in AMI model (Fig. 6D and E). Additionally, H&E staining showed that in the AMI group, myocardial cells in the border zone of the anterior wall infarct exhibited disordered arrangement and accumulation of

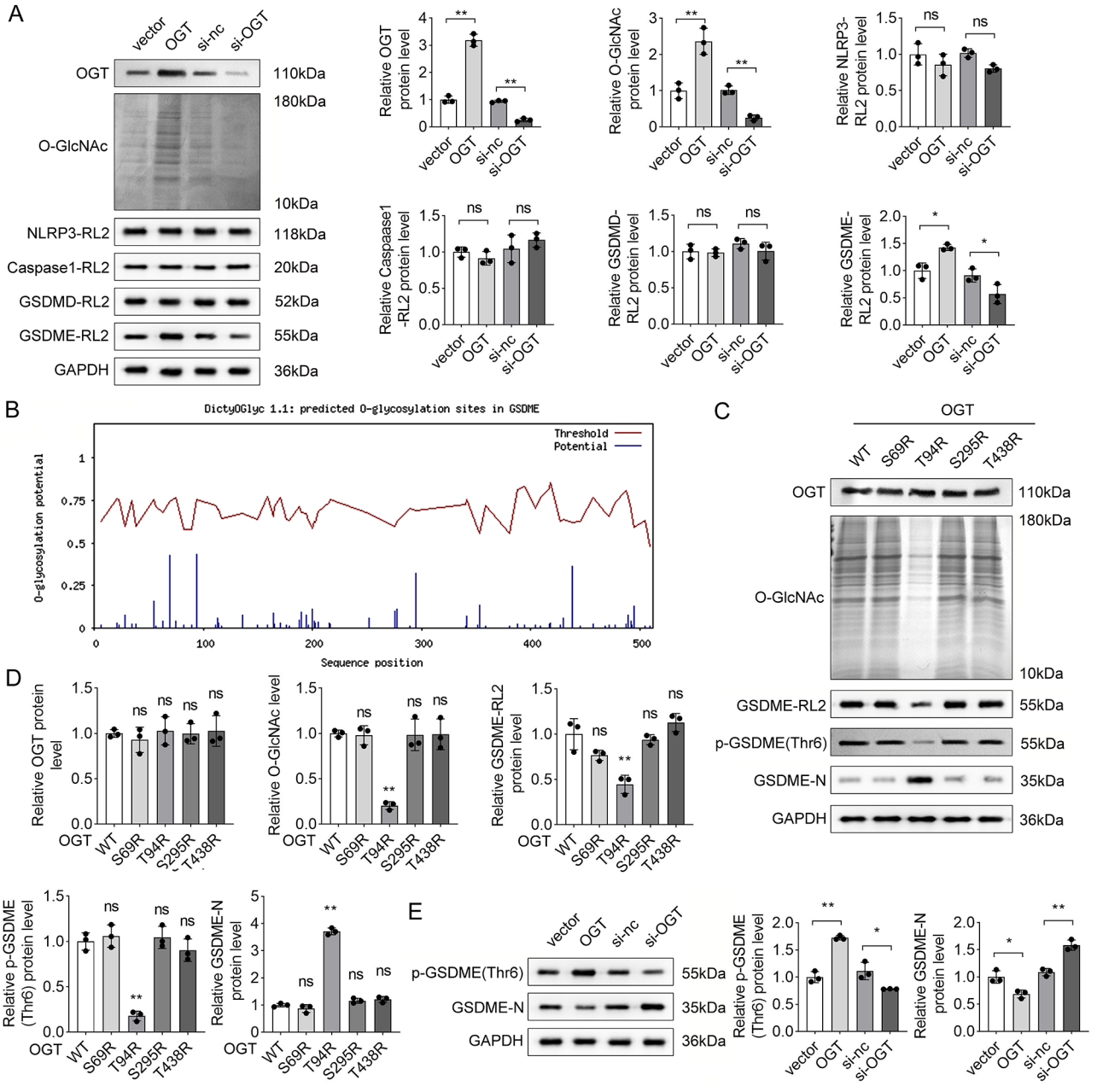

Fig. 5 OGT functioned as a suppressing factor for GSDME cleavage via increasing its O-GlcNAcylation. (**A**) Western blot was applied to identify the impacts of OGT overexpression and knockdown on the OGT and total O-GlcNAc levels, as well as O-GlcNAcylation modifications of NLRP3, caspase 1, GSDMD and GSDME. (**B**) The O-GlcNAcylation sites of GSDME predicted by GlycoMine website. (**C**, **D**) To ascertain the site of O-GlcNAcylation modification on GSDME, potential sites were mutated and then OGT, total O-GlcNAc, GSDME O-GlcNAcylation were assessed by western blot. (**E**) The phosphorylated and cleaved GSDME levels mediated by OGT were also determined with western blot. RL-2, O-GlcNAc; si-nc, small interfering RNA negative control; si-OGT, small interfering RNA targeting OGT; WT, wild-type; p-GSDME(Thr6), phosphorylation of GSDME at Thr6 site; GSDME-N, GSDME-N-terminal domain. $^{**}P < 0.01$. $^{*}P < 0.05$. ns: no significance

inflammatory cells with irregular distribution. Administration of kaempferol alleviated these symptoms in the myocardial tissues of AMI mice (Fig. 6F). Furthermore, the protein levels of OGT and the phosphorylation level of GSDME were decreased, while NLRP3 and GSDME-N were increased in the myocardial tissues of AMI mice. Administration of Kaempferol increased the OGT levels, decreased the NLRP3 and GSDME-N levels (Fig. 6G and H).

Discussion

AMI occupies approximately 14–20% of total cardiovascular diseases, which is second only to cancer as a high-risk disease [29]. Moreover, AMI is one of the leading

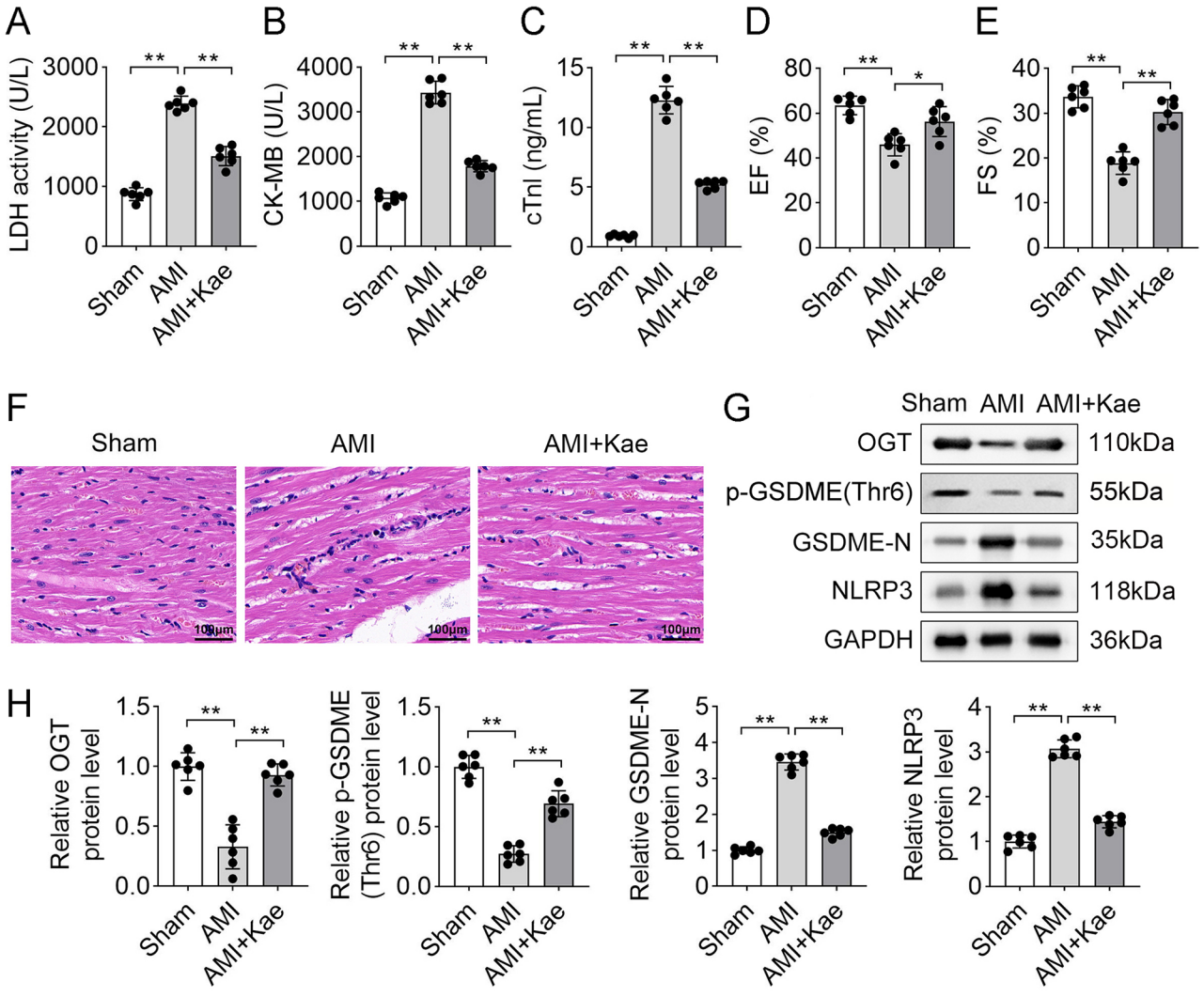

Fig. 6 Kaempferol alleviated the AMI progression in vivo. (**A**) LDH, (**B**) CK-MB and (**C**) cTnI levels in the myocardial tissues were detected by kits. (**D**) EF and (**E**) FS were measured using transthoracic echocardiography to evaluate the cardiac function of mice. (**F**) H&E staining of myocardial tissues. Scale bar: 100 μm. magnification: 40×. (**G**) Protein levels of OGT, p-GSDME(Thr6), GSDME-N and NLRP3 in the myocardial tissues were detected by western blot. (**H**) The protein levels were quantified by grey analysis. LDH, lactate dehydrogenase; CK-MB, creatine kinase MB isoenzyme; cTnI, cardiac troponin I; EF, ejection fraction; FS, fractional shortening; H&E, Hematoxylin-Eosin; p-GSDME(Thr6), phosphorylation of GSDME at Thr6 site; GSDME-N, GSDME-N-terminal domain. $^{**}P < 0.01$. $^{*}P < 0.05$

causes of global death and is considered a serious obstacle to public health [30]. It has been shown that H/R resulting from ischemia is closely associated with inflammation, oxidative stress and pyroptosis [31]. Multiple studies expound that H/R-induced myocardial damage is the dominating contributor to AMI. Considering that the pathogenesis of AMI is blurry, we established the classical H/R injury model in H9c2 cells and AMI mice model using permanent LAD ligation to investigate the latent molecular mechanism of AMI progression.

Pyroptosis is a type of cell death caused by numerous danger signals and serves as a core participant in the pathological development of AMI [32, 33]. A growing number of researche elucidate that AM-induced myocardial injury leads to the augment of pyroptosis [34]. It is extensively documented that Kaempferol plays a vital role in cell pyroptosis [35, 36]. Notably, a recent study has illustrated that Kaempferol alleviates myocardial damage in AMI via inhibition of pyroptosis [25]. Therefore, the goal of this study is to verify the potency of Kaempferol and inquire its regulatory mechanism in H/R-treated H9c2 cells to develop new strategies for the treatment of AMI. Herein, we justified that H/R stimulation contributed to the reduction of cell viability, the enhancement of LDH, IL-1β and IL-18 expression as well as the promotion of cell pyroptosis. Kaempferol attenuated H/R injury in H9c2 cells.

It is well known that glycosylation is a type of protein post-transcriptional modifications, which regulates protein folding, distribution and stability [37]. O-GlcNAcylation is an atypical glycosylation, which is reversible, dynamic and balanced in the coordination of OGT and OGA [38]. Increasing evidence has demonstrated that O-GlcNAcylation controls the activity and function of target proteins through rapid response to diverse stimulus signals [39]. Thus, O-GlcNAcylation is involved in the pathogenesis of various diseases, especially in AMI [40, 41]. More importantly, O-GlcNAcylation has been validated to function as a participant in pyroptosis [42]. Herein, we found that O-GlcNAcylation was suppressed by H/R treatment and then recovered by administration of Kaempferol. However, Kaempferol failed to restore the level of O-GlcNAc in H/R-induced cells to that of the control group, suggesting that Kaempferol may regulate pyroptosis through mechanisms other than O-GlcNAcylation, which needs further study. In agreement with reported literatures [43], H/R lowered OGT level and heighten OGA expression, while Kaempferol led to the restoration of OGT expression. Moreover, molecular docking revealed the binding of Kaempferol with OGT, which indicated that OGT might mediate the function of Kaempferol. Further investigations confirmed that knockdown of OGT abolished the inhibitory role of Kaempferol in cell pyroptosis.

GSDMD and GSDME are crucial factors that involved in pyroptosis. GSDMD is traditionally recognized as the primary executor of pyroptosis activated by caspase-1/4/5/11, while GSDME is typically cleaved by caspase-3 and has been implicated in the transition from apoptosis to pyroptosis [44]. A previous study has indicated that GSDMD regulates cardiomyocyte pyroptosis and thus promotes myocardial ischamis-reperfusion injury [45]. Another study also reported that GSDME-mediates myocardial cell pyroptosis is involved in AMI [46]. Of note, it was uncovered that OGT acted as a positive regulator for GSDME O-GlcNAcylation, but did not affect GSDMD O-GlcNAcylation. Hence, we focused on the role of GSDME in this study. Based on the O-GlcNAcylation sites predicted by bioinformatics, we demonstrated that OGT mediated the O-GlcNAcylation of GSDME at T94. It is acknowledged that phosphorylation is a major post-translational modification and participated in a wide range of cellular processes, including pyroptosis [47]. Further, early research has confirmed that O-GlcNAcylation can regulate protein phosphorylation through competing for the same serine/threonine, suggesting a competitive relationship between the two modifications [48]. However, emerging evidence validates that there is also a synergy between O-GlcNAcylation and phosphorylation, and mutating O-GlcNAcylation sites can inhibit protein phosphorylation [49, 50]. In this study, we observed that OGT contributed to GSDME phosphorylation and decreased the expression of GSDME-N. Notably, it has been illustrated that GSDME phosphorylation at Thr6 impedes the recognition of GSDME by caspase 3 to restrain GSDME cleavage and subsequent oligomerization of GSDME-N, thus inhibiting the pore-forming activity of GSDME and cell pyroptosis [51]. Considering these facts, we conjectured that Kaempferol might facilitate GSDME phosphorylation to suppress its cleavage through enhancing OGT-mediated O-GlcNAcylation, thereby reducing cell pyroptosis. In the future, we will conduct more investigations to confirm this theory.

A limitation of this study is the use of H9c2 myoblast cell line, which is different from cardiomyocytes. Although this cell line possesses multiple characteristics of cardiomyocytes, it simultaneously expresses calcium channels of both the heart and skeletal muscle. Therefore, it is necessary to use primary isolated cardiomyocytes to further verify our conclusion [52].

In conclusion, our study illuminated that Kaempferol repressed pyroptosis to improve H/R-induced injury through promoting OGT-mediated O-GlcNAcylation and phosphorylation of GSDME, and relieved the AMI progression in mice. These results clarified the novel regulatory mechanism of Kaempferol in AMI and supported the theoretical basis for its clinical application in cardiology.

Supplementary Information

The online version contains supplementary material available at https://doi.org/10.1186/s40360-025-00908-0.

Supplementary Material 1: Figure S1. Kaempferol Hypoxia/Reoxygenation, necrosis, and autophagy. (A) H9c2 cells were treated with Kaempferol or not, and western blot was conducted to measure the levels of proteins related to apoptosis (caspase3 and PARP1), necrosis (RIPK1 and RIPK3), and autophagy (LC3II and LC3I). (B) Quantitative analysis of western blot results. ns: no significance. CON, control; Kae, Kaempferol

Supplementary Material 2

Acknowledgements

Not applicable.

Author contributions

All authors participated in the design, interpretation of the studies and analysis of the data and review of the manuscript. Jie Zhou drafted the work and revised it critically for important intellectual content; Huifei Zhou and Jianfeng Zhu were responsible for the acquisition, analysis and interpretation of data for the work; Jie Zhou and Shunjin Fang made substantial contributions to the conception or design of the work. All authors read and approved the final manuscript.

Funding

The authors declare that no funds, grants, or other support were received during the preparation of this manuscript.

Data availability

The datasets used and/or analysed during the current study are available from the corresponding author on reasonable request.

Declarations

Ethics approval and consent to participate
This study was approved by the Ethics Committee of Huzhou Third Municipal Hospital. All animal experiments should comply with the ARRIVE guidelines. All methods were carried out in accordance with relevant guidelines and regulations.

Consent for publication
Not applicable.

Competing interests
The authors declare no competing interests.

Received: 26 September 2024 / Accepted: 19 March 2025
Published online: 08 April 2025

References

1. Reed GW, Rossi JE, Cannon CP. Acute myocardial infarction. Lancet. 2017;389(10065):197–210.
2. Hausenloy DJ, Yellon DM. Myocardial ischemia-reperfusion injury: A neglected therapeutic target. J Clin Invest. 2013;123(1):92–100.
3. Caruntu F, Bordejevic DA, Buz B, Gheorghiu A, Tomescu MC. Independent predictors of in-hospital and 1-year mortality rates in octogenarians with acute myocardial infarction. Rev Cardiovasc Med. 2021;22(2):489–97.
4. Moran AE, Forouzanfar MH, Roth GA, Mensah GA, Ezzati M, Flaxman A, et al. The global burden of ischemic heart disease in 1990 and 2010: The global burden of disease 2010 study. Circulation. 2014;129(14):1493–501.
5. Raskovalova T, Twerenbold R, Collinson PO, Keller T, Bouvaist H, Folli C, et al. Diagnostic accuracy of combined cardiac troponin and copeptin assessment for early rule-out of myocardial infarction: A systematic review and meta-analysis. Eur Heart J Acute Cardiovasc Care. 2014;3(1):18–27.
6. Macut D, Ognjanovic S, Asanin M, Krljanac G, Milenkovic T. Metabolic syndrome and myocardial infarction in women. Curr Pharm Des. 2021;27(36):3786–94.
7. Sun W, Gholizadeh L, Perry L, Kang K. Predicting return to work following myocardial infarction: A prospective longitudinal cohort study. Int J Environ Res Public Health. 2022;19(13).
8. Yang J, Yang XS, Zhang Q, Zhuang X, Dong XK, Jiang YH, et al. Down-regulated LINC01614 ameliorates hypoxia/reoxygenation-stimulated myocardial injury by directly sponging microRNA-138-5p. Dose Response. 2020;18(1):710604678.
9. Sharifi-Rad M, Fokou P, Sharopov F, Martorell M, Ademiluyi AO, Rajkovic J, et al. Antiulcer agents: From plant extracts to phytochemicals in healing promotion. Molecules. 2018;23(7).
10. Calderon-Montano JM, Burgos-Moron E, Perez-Guerrero C, Lopez-Lazaro M. A review on the dietary flavonoid Kaempferol. Mini Rev Med Chem. 2011;11(4):298–344.
11. Imran M, Salehi B, Sharifi-Rad J, Aslam GT, Saeed F, Imran A, et al. Kaempferol: A key emphasis to its anticancer potential. Molecules. 2019;24(12).
12. Vishwakarma A, Singh TU, Rungsung S, Kumar T, Kandasamy A, Parida S, et al. Effect of Kaempferol pretreatment on myocardial injury in rats. Cardiovasc Toxicol. 2018;18(4):312–28.
13. Zhou M, Ren H, Han J, Wang W, Zheng Q, Wang D. Protective effects of Kaempferol against myocardial ischemia/reperfusion injury in isolated rat heart via antioxidant activity and inhibition of glycogen synthase Kinase-3beta. Oxid Med Cell Longev. 2015;2015:481405.
14. Kamisah Y, Jalil J, Yunos NM, Zainalabidin S. Cardioprotective properties of Kaempferol: A review. Plants (Basel). 2023;12(11).
15. Bergsbaken T, Fink SL, Cookson BT. Pyroptosis: Host cell death and inflammation. Nat Rev Microbiol. 2009;7(2):99–109.
16. Labbe K, Saleh M. Cell death in the host response to infection. Cell Death Differ. 2008;15(9):1339–49.
17. Sollberger G, Strittmatter GE, Garstkiewicz M, Sand J, Beer HD. Caspase-1: The inflammasome and beyond. Innate Immun. 2014;20(2):115–25.
18. Xue Y, Enosi TD, Tan WH, Kay C, Man SM. Emerging activators and regulators of inflammasomes and pyroptosis. Trends Immunol. 2019;40(11):1035–52.
19. Toldo S, Mauro AG, Cutter Z, Abbate A. Inflammasome, pyroptosis, and cytokines in myocardial ischemia-reperfusion injury. Am J Physiol Heart Circ Physiol. 2018;315(6):H1553–68.
20. Toldo S, Abbate A. The NLRP3 inflammasome in acute myocardial infarction. Nat Rev Cardiol. 2018;15(4):203–14.
21. Liu W, Shen J, Li Y, Wu J, Luo X, Yu Y, et al. Pyroptosis inhibition improves the symptom of acute myocardial infarction. Cell Death Dis. 2021;12(10):852.
22. Chen S, Ma J, Yang L, Teng M, Lai ZQ, Chen X, et al. Anti-glioblastoma activity of Kaempferol via programmed cell death induction: Involvement of autophagy and pyroptosis. Front Bioeng Biotechnol. 2020;8:614419.
23. Cai M, Zhuang W, Lv E, Liu Z, Wang Y, Zhang W, et al. Kaemperfol alleviates pyroptosis and microglia-mediated neuroinflammation in Parkinson's disease via inhibiting p38MAPK/NF-kappaB signaling pathway. Neurochem Int. 2022;152:105221.
24. Liu Z, Yao X, Sun B, Jiang W, Liao C, Dai X, et al. Pretreatment with Kaempferol attenuates microglia-mediate neuroinflammation by inhibiting MAPKs-NF-kappaB signaling pathway and pyroptosis after secondary spinal cord injury. Free Radic Biol Med. 2021;168:142–54.
25. Hua F, Li JY, Zhang M, Zhou P, Wang L, Ling TJ, et al. Kaempferol-3-O-rutinoside exerts cardioprotective effects through NF-kappaB/NLRP3/Caspase-1 pathway in ventricular remodeling after acute myocardial infarction. J Food Biochem. 2022;46(10):e14305.
26. Ma M, Liang SC, Diao KY, Wang Q, He Y. Mitofilin mitigates myocardial damage in acute myocardial infarction by regulating pyroptosis of cardiomyocytes. Front Cardiovasc Med. 2022;9:823591.
27. Yang C, Yang W, He Z, He H, Yang X, Lu Y, et al. Kaempferol improves lung Ischemia-Reperfusion injury via antiinflammation and antioxidative stress regulated by SIRT1/HMGB1/NF-kappaB axis. Front Pharmacol. 2019;10:1635.
28. Panda S, Pradhan N, Chatterjee S, Morla S, Saha A, Roy A, et al. 4,5-Disubstituted 1,2,3-triazoles: Effective inhibition of indoleamine 2,3-Dioxygenase 1 enzyme regulates T cell activity and mitigates tumor growth. Sci Rep. 2019;9(1):18455.
29. Anderson JL, Morrow DA. Acute myocardial infarction. N Engl J Med. 2017;376(21):2053–64.
30. Mozaffarian D, Benjamin EJ, Go AS, Arnett DK, Blaha MJ, Cushman M, et al. Heart disease and stroke statistics–2015 update: A report from the American heart association. Circulation. 2015;131(4):e29–322.
31. Zhang BH, Liu H, Yuan Y, Weng XD, Du Y, Chen H, et al. Knockdown of TRIM8 protects HK-2 cells against hypoxia/reoxygenation-induced injury by inhibiting oxidative stress-mediated apoptosis and pyroptosis via PI3K/Akt signal pathway. Drug Des Devel Ther. 2021;15:4973–83.
32. Yuan J, Najafov A, Py BF. Roles of caspases in necrotic cell death. Cell. 2016;167(7):1693–704.
33. Naryzhnaya NV, Maslov LN, Popov SV, Mukhomezyanov AV, Ryabov VV, Kurbatov BK, et al. Pyroptosis is a drug target for prevention of adverse cardiac remodeling: The crosstalk between pyroptosis, apoptosis, and autophagy. J Biomed Res. 2022;36(6):375–89.
34. Qiu Z, He Y, Ming H, Lei S, Leng Y, Xia ZY. Lipopolysaccharide (LPS) aggravates high glucose- and hypoxia/reoxygenation-induced injury through activating ROS-Dependent NLRP3 inflammasome-mediated pyroptosis in H9C2 cardiomyocytes. J Diabetes Res. 2019;2019:8151836.
35. Huang X, Wang Y, Yang W, Dong J, Li L. Regulation of dietary polyphenols on cancer cell pyroptosis and the tumor immune microenvironment. Front Nutr. 2022;9:974896.
36. He C, Yang J, Jiang X, Liang X, Yin L, Yin Z, et al. Kaempferol alleviates LPS-ATP mediated inflammatory injury in splenic lymphocytes via regulation of the pyroptosis pathway in mice. Immunopharmacol Immunotoxicol. 2019;41(5):538–48.
37. Jayaprakash NG, Surolia A. Role of glycosylation in nucleating protein folding and stability. Biochem J. 2017;474(14):2333–47.
38. Yang X, Qian K. Protein O-GlcNAcylation: Emerging mechanisms and functions. Nat Rev Mol Cell Biol. 2017;18(7):452–65.
39. Fisi V, Miseta A, Nagy T. The role of stress-induced O-GlcNAc protein modification in the regulation of membrane transport. Oxid Med Cell Longev. 2017;2017:1308692.
40. Zuurbier CJ, Bertrand L, Beauloye CR, Andreadou I, Ruiz-Meana M, Jespersen NR, et al. Cardiac metabolism as a driver and therapeutic target of myocardial infarction. J Cell Mol Med. 2020;24(11):5937–54.
41. Wang D, Hu X, Lee SH, Chen F, Jiang K, Tu Z, et al. Diabetes exacerbates myocardial ischemia/reperfusion injury by Down-Regulation of MicroRNA and Up-Regulation of O-GlcNAcylation. JACC Basic Transl Sci. 2018;3(3):350–62.
42. Yang H, Xiao L, Wu D, Zhang T, Ge P. O-GlcNAcylation of NLRP3 contributes to lipopolysaccharide-induced pyroptosis of human gingival fibroblasts. Mol Biotechnol. 2024;66(8):2023–31.

43. She C, Zhu J, Liu A, Xu Y, Jiang Z, Peng Y. Dexmedetomidine inhibits NF-kappaB-Transcriptional activity in neurons undergoing ischemia-reperfusion by regulating O-GlcNAcylation of SNW1. J Neuropathol Exp Neurol. 2022;81(10):836–49.
44. Shi J, Gao W, Shao F, Pyroptosis. Gasdermin-Mediated programmed necrotic cell death. Trends Biochem Sci. 2017;42(4):245–54.
45. Shi H, Gao Y, Dong Z, Yang J, Gao R, Li X, et al. GSDMD-mediated cardiomyocyte pyroptosis promotes myocardial I/R injury. Circ Res. 2021;129(3):383–96.
46. Li Y, Wang X, Meng X, Xia C, Yang C, Wang J, et al. Aerobic exercise inhibits GSDME-dependent myocardial cell pyroptosis to protect ischemia-reperfusion injury. Mol Med. 2024;30(1):273.
47. Swanson KV, Deng M, Ting JP. The NLRP3 inflammasome: Molecular activation and regulation to therapeutics. Nat Rev Immunol. 2019;19(8):477–89.
48. Love DC, Hanover JA. The hexosamine signaling pathway: Deciphering the O-GlcNAc code. Sci STKE. 2005;2005(312):e13.
49. Hu P, Shimoji S, Hart GW. Site-specific interplay between O-GlcNAcylation and phosphorylation in cellular regulation. FEBS Lett. 2010;584(12):2526–38.
50. Kakade PS, Budnar S, Kalraiya RD, Vaidya MM. Functional implications of O-GlcNAcylation-dependent phosphorylation at a proximal site on keratin 18. J Biol Chem. 2016;291(23):12003–13.
51. Ai YL, Wang WJ, Liu FJ, Fang W, Chen HZ, Wu LZ, et al. Mannose antagonizes GSDME-mediated pyroptosis through AMPK activated by metabolite GlcNAc-6P. Cell Res. 2023;33(12):904–22.
52. Mejia-Alvarez R, Tomaselli GF, Marban E. Simultaneous expression of cardiac and skeletal muscle isoforms of the L-type Ca2 + channel in a rat heart muscle cell line. J Physiol. 1994;478(Pt 2):315–29.

Publisher's note